

# Optimization of the Aerodynamics Airfoils Placed in Supersonic Viscous Flow

Victorița Rădulescu

University Politehnica of Bucharest/Hydraulics, Hydraulic machinery and Environmental Engineering,  
Bucharest, Romania, e-mail: vradul4@gmail.com

**Abstract** – Nowadays the efficiency of aerodynamics profiles placed in a supersonic flow represents a permanent goal of the human civil transportation or military equipments. Present paper intends to present an optimization method of their shapes, taking into account the Navier-Stokes flow equations, applied for thin layers. Generally, in supersonic flow, the cross-sections of the wings are thin profiles, symmetric as to reduce the drag force coefficient and maximize the lift coefficient. It is presented a method of the shape calculation for aerodynamic profiles with small curvature, based on integral equations Fredholm of the second kind, with a good behavior in the supersonic flows. Some aspects referring to the unsteady flows and air compressibility are also mentioned. There were selected four aerodynamic airfoils with characteristics dedicated to high velocities, with different characteristics, having as main purpose the identification of essential aspects needed to be considered in the numerical modeling. From these four profiles, two are deduced by theoretical assessments, and two are special known as super-sonic aerodynamic profiles. They were first tested into a subsonic wind channel for incidences between  $0^\circ - 4^\circ$  at different values of wind velocity and secondly into a supersonic wind tunnel, at same incidences, as to better analyze the main factors who influence the aerodynamic of shapes curvature and to assure an optimization of their behavior. The purpose of testing these profiles was to improve the main characteristics, especially into the trailing and leading edges. The effect of the angle of attack, the influence of velocity and viscosity, the shape curvature on the vortex development were also considered. The obtained results assure a better functioning in the supersonic flow regime, eliminating the adverse pressure gradient and the boundary layer separation, assuring an optimum behavior. Finally are mentioned some conclusions and references.

**Cuvinte cheie:** TLNS – Ecuatiile Navier-Stokes in filme subtiri,  $C_{d,p}$ -coeficient de presiune,  $C_{d,s}$ -coeficient de forma,  $v_\infty$ -viteza curentului principal, eficienta formei profilului aerodinamic.

**Keywords:** TLNS - the Thin Layer Navier-Stokes equations,  $C_{d,p}$ -pressure drag coefficient,  $C_{d,s}$ -skin-friction drag,  $v_\infty$ -upstream velocity, aerodynamic shape efficiency.

## I. INTRODUCTION

The recent interest in the high-speed civil transport is renewed by the research for the enhanced supersonic configuration of the aerodynamic airfoils. To improve the efficiency of such aircraft, it is necessary to assure an optimization of the wing sections, formed by aerodynamics profiles, vital in the fuel economy during flights and transport capacity. Due to the vortices, which are, sepa-

rating from the wing with infinite development, new problems concerning the space, flight corridors, environmental protection, must be solved as efficient as possible.

In the past, as first step [1], were assumed the linear equations to model the airflow around aircraft and to develop the basic concepts. In this case was imposed a thickness constraint to optimize the shape for a double-wedge profile. As second step [2] were introduced the non-linear equations, taking into account the effect of viscosity. In this case, the obtained shape was slightly shifted, with the maximum thickness location in the flow direction. It must be mentioned that generally the maximum thickness location is around the 0.4-mid chore, and the leading and trailing edges are sharp.

In actual researches are introduced the three-dimensional effects of the airflow, but the made analysis were mainly for subsonic flow. First step is to assume the conical full potential approach [3], with immediate effect the modification of the linearization theory [4], [5] for the fluid flow equations.

Firstly, in the present paper is briefly mentioned a method of solving the main aspects of flow around profiles with small curvature, based on Fredholm integral equations of second kind, followed by an estimation of the drag and lift coefficients.

It is also introduced the effect of viscous nature of the fluid flow, based on previous investigations [6] having as main purpose an optimization of the profile thickness. It must be mentioned that in subsonic movements [7], appears a flow expanding around the leading edge, starting from the stagnation point. There are mentioned some possibilities to reduce the drag coefficient, taking into account its components due to the pressure distribution (the drag coefficient component), due to the fluid compressibility or the shock component, and due to the fluid viscosity.

Many problems connected to supersonic transport are associated with the shock waves due to the vortices, due to the sonic boom or due to the influence of the shape of wings on the kerosene consumption, upper atmospheric environmental problems, sideline noise, the vortex hazard expanding, etc. All these aspects impose an improvement of the aerodynamic wing performance, especially at this range of speed.

The numerical modeling of the wing has the main purpose the designing and achievement of a desired load and pressure distribution along the leading edge. Additional must be assured a cambered and twisted vortex after leaving the airfoil, aligned to the local flow direction [8]. In each case, a proper attack-angle should be considered. The results of considering the air viscosity in the leading edge area has as immediate result a very high suction pressure,

with separation of the boundary layer, along the swept separation line. For the free stream flow, as initial conditions, are selected the no-slip conditions and the adiabatic condition for air structure.

## II. THEORETICAL ASPECTS IN AERODYNAMICS ESTIMATION OF THIN PROFILES

Generally, the previous theoretical and experimental tests proved that in supersonic flows is better to be used airfoils with simple geometry, being more efficient (for instance, the diamond, or profile formed as combination of arc curvature). Nowadays, due to the aspects requiring the minimization of the drag coefficient and due to the decreasing of the vortices development, the profile shape with low curvature became more adequate. The remaining problems consist in the proper shape, thickness, and values of the incidence angle of attack.

Further is presented a method based on Fredholm integral equations of second kind in estimation the profile shape. The method is applied to profiles with smooth surface with low curvature, rounded but with very thin trailing edge. Subsequently will be presented the corrections for the profile with sharp trailing edge. As a first approximation is considered that, there is no flow separation and the profile is a streamline. The velocity on profile C may be expressed:

$$\bar{v}(z) = -\frac{1}{2\pi i} \int_C \bar{v}(\zeta) H(\zeta, z) d\zeta + \bar{v}_\infty \quad (1)$$

Where the nucleus is:

$$H(\zeta, z) = \frac{1}{\zeta - z} + 2(\zeta - z) \sum_{k=1}^{\infty} \frac{1}{(\zeta - z)^{2k}}$$

After few calculations and considering the component of the induced velocity on profile  $v_{\Gamma_x}(s, \sigma)$ ,  $v_{\Gamma_y}(s, \sigma)$  into a point by the infinite small vortices we obtain an integral equation Fredholm second kind with continuous nucleus:

$$\begin{aligned} v(s) - 2 \int_C \bar{v}(\sigma) [v_{\Gamma_x}(s, \sigma) \cos \nu(s) + v_{\Gamma_y}(s, \sigma) \sin \nu(s)] d\sigma = \\ = 2[v_{\infty x} \cos \nu(s) + v_{\infty y} \sin \nu(s)] \end{aligned} \quad (2)$$

Considering the auxiliary angle  $\phi$  for the fix point by coordinates  $x(\phi)$ ,  $y(\phi)$  and angle  $\psi$  for the current point by coordinates  $\xi(\sigma)$ ,  $\eta(\sigma)$  and with notations:

$$\begin{aligned} s(\phi) &= \sqrt{x(\phi)^2 + y(\phi)^2} & \sigma(\psi) &= \sqrt{x(\psi)^2 + y(\psi)^2} \\ \omega(\phi) &= v(s) \cdot s(\phi) & \omega(\psi) &= v(\sigma) \cdot \sigma(\psi) \end{aligned}$$

Eq. (1) became:

$$\omega(\phi) - \frac{1}{\pi} \int_0^{2\pi} \omega(\psi) K(\phi, \psi) d\psi = 2[v_{\infty x} x(\phi) + v_{\infty y} y(\phi)] \quad (3)$$

Where the nucleus is:

$$K(\phi, \psi) = \frac{[x(\phi) - x(\psi)] \cdot y(\phi) - [y(\phi) - y(\psi)] \cdot x(\phi)}{[x(\phi) - x(\psi)]^2 + [y(\phi) - y(\psi)]^2} \quad (4)$$

Relation (4) may be reduced to a linear dependent system, with M unknown and M equations. For thin profiles, the number of equations must be  $M \geq 25$ .

For profiles with angular leading edge, it must be imposed an additional condition

$$\sum_{\nu=2}^M K_\nu \omega_\nu = -M(v_{\infty x} \cos \beta_L + v_{\infty y} \sin \beta_L) \quad (5)$$

Where  $\beta_L$  is the angle into the leading edge. The profile curvature may be deduced from the relation:

$$\frac{dy_f}{dx} = \frac{v_{\infty y} + v_{iy}(x)}{v_{\infty x} + v_{ix}(x)} \quad (6)$$

Where  $v_{ix}$ ,  $v_{iy}$  are the components of the vortices induced by profile asymmetry, responsible for the vortex development, analyzed in paragraph 3 and by the attack angle. The profile thickness may be deduced from the relation, taking into account that  $q(x)$  is the induced flow by de presence of the profile:

$$\frac{dy_d}{dx} = \frac{q(x)}{2(v_{\infty x} + v_{ix})} \quad (7)$$

For further developments, as to reduce the drag coefficient and to study the vortices development, it must be deduced the velocity on the upper surface  $v^+$  and respectively  $v^-$  on the lower surface,

$$\begin{aligned} \frac{v^\pm}{v_{\infty x}} &= \frac{1}{\sqrt{1 + \left(\frac{dy_d}{dx}\right)^2}} \left\{ 1 + \frac{A_0}{2} \left( \pm \operatorname{ctg} \frac{\theta}{2} + v_x \right) + \right. \\ &+ \frac{B_0}{2} (1 + 2 \cos \theta + v_x) + \sum_{k=2}^{\infty} \frac{A_{k-1}}{2} (\pm \sin(k-1)\theta + v_{x,k-1}) \\ &\left. + \frac{B_k}{2} (-\cos k\theta + v_{xk}) \right\} \quad 0 < \theta \leq \pi \end{aligned} \quad (8)$$

Where  $A_0 \dots A_k$ ,  $B_0 \dots B_k$  are the influence coefficients.

The lift coefficient may be written:

$$C_L = 2\pi \left[ \left( \frac{A_0}{2} + \frac{A_1}{2} \right) \cos \alpha_\infty + \left( \frac{A_0}{2} + \frac{A_1}{4} \right) \sin \alpha_\infty \right] \quad (9)$$

## III. FLOW EQUATIONS FOR COMPRESSIBLE FLUID FLOW IN SUBSONIC CONDITIONS

There were tested two profiles in subsonic flow, with optimization taking into account the viscosity effect and the normal attack-angle for the wing.

The method of optimization couple the computational fluid dynamics equations with the sensitivity aspects, introduced in 1995 [9]. The step size representing the incremental variable changes in the design for optimal shapes was not kept constant as in the previously mentioned papers. Each new step is based on the previous design, with corrections referring at viscosity and a new attack-angle. The flow field analysis and the evaluation of constrains were obtained by solving the Thin-Layer Navier-Stokes equations (TLNS).

The unsteady boundary-layer equation can be formally derived by neglecting the small terms. As consequence, all viscous terms containing derivatives parallel to the body surface are dropped since they are substantially smaller than viscous terms containing derivatives normal to the

surface. In addition, the momentum equation is reduced to a simpler equation [10].

The viscous terms containing derivatives in the direction parallel to the airfoil surface are again neglected, but all terms in the momentum equation are retained.

This concept of thin-layer approximation arises from a detailed examination of typical high Reynolds numbers computations involving the complete Navier-Stokes (N-S) equations. Upon simplifying the complete N-S equations using TLNS, the main equations become:

- Continuity (mass conservation)

$$\frac{\partial \rho}{\partial t} + \frac{\partial(\rho v_x)}{\partial x} + \frac{\partial(\rho v_y)}{\partial y} + \frac{\partial(\rho v_z)}{\partial z} = 0 \quad (10)$$

- x - Momentum

$$\frac{\partial(\rho v_x)}{\partial t} + \frac{\partial}{\partial x}(p + \rho v_x^2) + \frac{\partial}{\partial y}(\rho v_x v_y - \mu \frac{\partial v_x}{\partial y}) + \frac{\partial}{\partial z}(\rho v_x v_z) = 0$$

- y- Momentum

$$\frac{\partial(\rho v_y)}{\partial t} + \frac{\partial}{\partial x}(\rho v_x v_y) + \frac{\partial}{\partial y}(p + \rho v_y^2 - \frac{4}{3} \mu \frac{\partial v_y}{\partial y}) + \frac{\partial}{\partial z}(\rho v_y v_z) = 0 \quad (11)$$

After some calculations, taking into account of the previous mentions, the equations (10), and (11) become:

$$\frac{\partial(\rho^* v_x^*)}{\partial x^*} + \frac{\partial(\rho^* v_y^*)}{\partial y^*} = 0(\varepsilon) \quad (12)$$

- x - Momentum

$$\rho^* v_x^* \frac{\partial v_y^*}{\partial x^*} + \rho^* v_y^* \frac{\partial v_x^*}{\partial y^*} = -\Delta^2 \frac{\partial p^*}{\partial x^*} + \frac{1}{(\delta^*)^2 \text{Re}_{ref}} \frac{\partial}{\partial y^*} \left( \mu^* \frac{\partial v_x^*}{\partial y^*} \right) + 0[\varepsilon, (\text{Re}_{ref})^{-1}] \quad (13)$$

- y - Momentum

$$\rho^* v_x^* \frac{\partial v_y^*}{\partial x^*} + \rho^* v_y^* \frac{\partial v_y^*}{\partial y^*} = -\left(\frac{\Delta}{\delta}\right)^2 \frac{\partial p^*}{\partial y^*} + \frac{1}{(\delta^*)^2 \text{Re}_{ref}} \left[ \frac{4}{3} \frac{\partial}{\partial y^*} \left( \mu^* \frac{\partial v_y^*}{\partial y^*} \right) + \frac{\partial}{\partial x^*} \left( \mu^* \frac{\partial v_x^*}{\partial y^*} \right) - \frac{2}{3} \frac{\partial}{\partial y^*} \left( \mu^* \frac{\partial v_x^*}{\partial x^*} \right) \right] + 0[\varepsilon, (\text{Re}_{ref})^{-1}]$$

The first term in the series expansion is used to obtain the zero order solution, while both first and second terms are needed to obtain the first order solution. The normal gradient to the surface is much greater than the gradient parallel to the surface; this one may be neglected.

An initial starting solution is required for the leading edge problem. For the present problem, profiles with small thickness and curvature, it is permissible to use an appropriate starting solution located very close to the leading edge, because it will have a small effect on the flow field in the further downstream.

As a result, the equations behave in a strictly "parabolic" manner in the boundary-layer region. The coordinated x, y, z are made non-dimensional by using L,  $\delta_y$ ,  $\delta_z$  and also the velocity components  $v_x$ ,  $v_y$ ,  $v_z$ , are non-dimensional using  $V_\infty$ ,  $V_\infty \delta_y^*$ ,  $V_\infty \delta_z^*$ , where  $\delta_y^* = \delta_y / L$

and  $\delta_z^* = \delta_z / L$ . Terms of  $(\delta_z^*)^2$ ,  $(\delta_y^*)^2$ ,  $\delta_y^* \delta_z^*$  are assumed to be very small and neglected.

The optimization method always tries to reduce the thickness of the profile within the limits of the geometric constrains. The compressibility produces changes in the flow patterns and in the resulting forces and moments.

Near the trailing edge appear some vortices who affect the chord wise pressure distribution (Fig.1). In addition to the leading edge, a second suction peak appears in this section. This one is associated with the vortex developed into the upper surface of the profile. The flow on this area is dominated by the pressure gradient between the profile and the suction sides.



Fig. 1. Appearance and development of vortices on extrados.

From the momentum equations, the viscous term will have only a secondary effect on the vortices flow and the further rolling-up. If the vortex continues downstream away from the airfoil, the pressure gradient is not dominant and the compressibility will take an important role.

The TLNS assumption is justified since these terms are substantially smaller than the terms with derivatives normal to the profile. In addition, it would be practical to think at a grid that could be refined enough in the direction parallel to the profile to resolve the diffusive terms in this direction. The solution of the TLNS set of equations has an advantage over the boundary-layer equations, which assume the normal pressure gradient negligible. Therefore, the TLNS equations are capable of handling the flow separation and the reverse flow regions with no special necessary considerations.

#### IV. FLOW EQUATIONS IN SUPERSONIC CONDITIONS

Taking account of dissipation's differences between pressure from extrados and intrados:

$$\frac{p_2 - p_1}{q_1} = \left\{ \frac{p_2}{p_1} \left[ 1 + \frac{M_1^2 \left( 1 - \frac{v_2^2}{v_1^2} \right)}{\frac{k+1}{k-1} - M_1^2} \right]^{\frac{k}{k-1}} - 1 \right\} / \left[ \left( 1 + \frac{M_1^2}{\frac{k+1}{k-1} - M_1^2} \right)^{\frac{k}{k-1}} - 1 \right] \quad (14)$$

If the Mach number increases, a local zone of supersonic flow may be developed and changes of pressure distribution appear significantly. The profile has some lift and therefore the extrados becomes super-sonic first.

The transition from subsonic to supersonic flow occurs smoothly but the transition back to subsonic flow appears

generally through a shock wave. When the local Mach number is  $>1$  the shock wave becomes strong and the pressure distribution is radically altered. The phenomenon is realized very quickly. If the Mach number is further increased, the shocks also develop on the intrados not only on extrados. The sudden increase of pressure distribution after the shock can cause the separation of the boundary layer with a substantial increase in the drag coefficient [11].

For potential 2D motions, the continuity equation (mass conservation) may be written:

$$\frac{1}{a^2} \vec{V} \cdot \text{grad} p + \rho \Delta \varphi = 0 \quad (15)$$

Respectively:

$$\frac{\partial^2 \varphi}{\partial x^2} \left(1 - \frac{v_x^2}{a^2}\right) + \frac{\partial^2 \varphi}{\partial y^2} \left(1 - \frac{v_y^2}{a^2}\right) - \frac{2v_x v_y}{a^2} \frac{\partial^2 \varphi}{\partial x \partial y} = 0 \quad (16)$$

The profile has small curvature and thickness, so the perturbations are small. The velocity components are:

$$v_x = v_\infty + v_x' \quad v_y = v_y' \quad (17)$$

Eq. (12) became

$$\frac{\partial^2 \varphi}{\partial x^2} (1 - M_\infty^2) + \frac{\partial^2 \varphi}{\partial y^2} = 0 \quad (18)$$

Respectively the velocity on the profile contour:

$$\frac{v^\pm(x)}{v_{\infty x}} = \frac{1}{\sqrt{1 + \left(\frac{dy_d}{dx}\right)^2}} \left[ 1 + \frac{1}{\sqrt{1 - M_\infty^2}} \left( \frac{v_{inc}^\pm(x)}{v_{\infty x}} - 1 \right) \right] \quad (19)$$

The Busemann relations for the pressure coefficient:

$$C_p = \frac{2\Theta}{\sqrt{Ma_\infty^2 - 1}} + \frac{(\gamma - 1)Ma_\infty^4 - 4M_\infty^2 + 4}{2(M_\infty^2 - 1)^2} \quad (20)$$

and for the lift and drag coefficients due to the attack angle and of thickness:

$$C_l = \frac{2\Theta}{\sqrt{M_\infty^2 - 1}} \quad (21)$$

$$C_d = \frac{4\alpha^2}{\sqrt{M_\infty^2 - 1}} + \frac{2}{\sqrt{M_\infty^2 - 1}} \int_0^1 \left[ \left( \frac{\partial v_x}{\partial x} \right)^2 + \left( \frac{\partial v_y}{\partial x} \right)^2 \right] dx$$

When  $\theta$  is positive, the flow is turned away from the downstream direction and when it is negative it is being turned to upstream direction.

The shock wave appearing at supersonic flow gradually moves back to the trailing edge and almost all of the airfoil is surrounded by a supersonic flow. In this condition, the drag coefficient increases very much and the airfoil operates far from the optimum point. Further increases in Mach number (supersonic incident flow) change the flow characteristic totally.

When the upstream flow is supersonic, the airfoil behavior is quite changed, because the supersonic flow is not able to suddenly change the direction when it happens onto the airfoil leading edge.

A bow wave is formed, extending far into the flow domain and only a small region near the airfoil remains subsonic. If the Mach number increases more, the bow wave is sent back and only a very small area near the trailing edge remains subsonic.

## V. EXPERIMENTAL AND NUMERICAL RESULTS

The measurements at subsonic velocity were accomplished into Aerodynamic Laboratory of the Department of Hydraulics, Hydraulic machinery and Environmental engineering from University Politehnica of Bucharest for the profiles NACA 0006 and NACA 0008 (Fig.2).

The supersonic measurements were realized at tunnel of INCAS institute for the profiles NACA 2S-3003-3003 and NACA 1S 5030-5030 (Fig.3). In Table 1, are mentioned their characteristics.

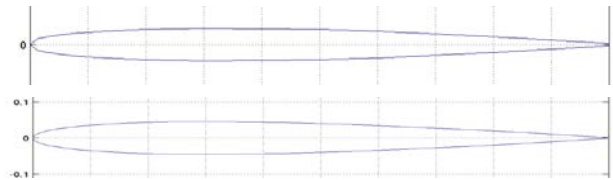


Fig. 2. Profiles NACA 0006 and NACA 0008.

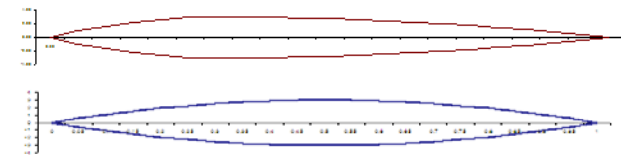


Fig. 3. Profiles for supersonic flows.

TABLE I. PROFILES CHARACTERISTICS

	NACA 0006	NACA 0008		NACA 2S-3003-3003	NACA 1S 5030-5030
1	0,00063	0,00084	1	0	0
0,95	0,00403	0,00537	0,95	0,92	0,57
0,9	0,00724	0,00965	0,9	1,67	1,08
0,8	0,01312	0,01749	0,85	2,25	1,53
0,7	0,01832	0,02443	0,8	2,67	1,92
0,6	0,02282	0,03043	0,75	2,92	2,25
0,5	0,02647	0,03529	0,7	3	2,52
0,4	0,02902	0,03869	0,65	2,98	2,73
0,3	0,03001	0,04001	0,6	2,94	2,88
0,25	0,02971	0,03961	0,55	2,86	2,97
0,2	0,02869	0,03825	0,5	2,75	3
0,15	0,02673	0,03564	0,45	2,61	2,97
0,1	0,2341	0,03121	0,4	2,45	2,88
0,075	0,021	0,028	0,35	2,25	2,73
0,05	0,01777	0,02369	0,3	2,02	2,52
0,025	0,01307	0,01743	0,25	1,76	2,25
0,125	0,00947	0,01263	0,2	1,47	1,92
0	0	0	0,15	1,15	1,53
			0,1	0,79	1,08
			0,05	0,4	0,57
			0	0	0

The Characteristics of the Supersonic Wind Tunnel:

- blow down type, 1,2 m x 1,2 m test section (3D)
- Mach number range 0,1–3,5
- Reynolds number up to 100 millions/m
- Max. test run duration: 90 sec
- Max. pressure 12 bar (settling chamber)

- Interchangeable 3D/2D 0.48m x 1.2m test section
- The Equipment from the supersonic Wind Tunnel:
  - Sting mounted, internal balance
  - TASK & TEM equipment
  - Home made profiles, Pressure measurements
  - Mach control system, IR ultra fast camera

There were selected 18 points on the extrados and 18 into the intrados. The side constraints for both surfaces were set to 0.5 and -0.5 of the normalized chord length. This type of set up was critical in mitigating the negative volume problems in grid regeneration during the optimization process.

The present study also demonstrates the possible difficulties in solving such optimization problems.

From experiments, we may observe an increasing of the wing lift for the curve slope when the Mach number grows. The  $C_L$  increases with the Mach number and reverses itself when strong shocks appear due to the wing shape. The drag coefficient increases with the Mach number. The obtained results for the drag coefficient  $C_d$ , for the selected profiles at different values of Mach number are presented (Fig.4). The drag coefficient increases with the Mach number at a given  $C_L$ . The data are based on measurements made in the supersonic tunnel.

In selection of the supersonic aircraft, the amount of sweep back in the lifting surfaces could affect the selection of the type of aerodynamic airfoils for those surfaces.

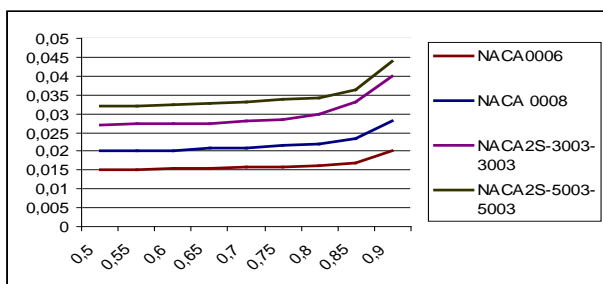


Fig. 4. Variation of  $C_d$  with Ma number for tested profiles.

If the component of the normal stream velocity in the leading edge on the extrados is subsonic, we may use profiles with rounded leading edge. If the normal component of the stream velocity is supersonic, it is necessary to select profiles with sharp leading edge, as to minimize the wave resistance. Another reason may be the stability and structural resistance as to limit the amount of sweepback.

For some flight-conditions, sometimes it is necessary to reduce the aircraft velocity; that was the reason why the profiles were tested also at subsonic conditions; it is necessary to evaluate the influence of thickness, of curvature of the sharp trailing edges in these conditions.

Further (Fig.5) are presented the obtained results for pressure coefficient  $C_p=f(l)$ , where  $l$  is the length chord profile for NACA 0006 at  $Ma=0.8$  and  $Ma=1.1$ . Other effects include a moving of the diagram of pressure that cause a nose-down pitching moment, and a rapid increase of the drag force as shocks form.

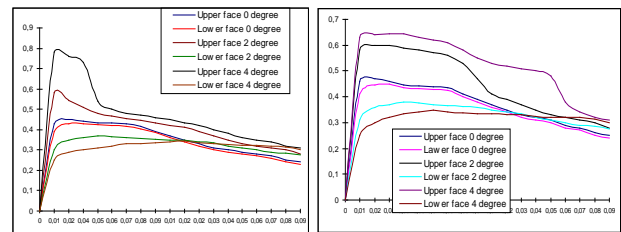


Fig. 5.  $C_p=f(l)$  for NACA 0006 at  $Ma = 0.8$  and  $Ma = 1.1$ .

For each profile were realized measures at three incidence angles:  $0^\circ$ ,  $2^\circ$ , and  $4^\circ$ . Next (Fig.6) are presented the obtained results for pressure coefficient, for profile NACA 2S-3003-3003 at the same Ma numbers,  $Ma = 0.8$  and  $Ma = 1.1$ .

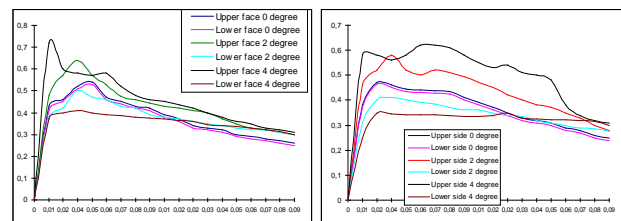


Fig. 6.  $C_p=f(l)$  for NACA 2S-3003-3003 at  $Ma = 0.8$  and  $Ma = 1.1$ .

By creating a network with flexible grid approach it is possible to observe that some grid lines of the same family may inadvertently cross each other due to the an inadequate grid parameters or to the undesirable inflexion points on the surface. To reduce the computer memory requirements, was used the sensitivity analysis with domain decomposition technique.

The present calculations use the code ADOS which includes all the movement equations. To perform the shape optimizations are necessary the following initial tasks:

1. Determination of the initial geometry shape of aerodynamic profile, and for the numerical modeling and testing were selected the mentioned profiles
2. Modification of subroutine, which requires changes, based on the particular problem, of TLNS
3. Obtaining the initial grid with variable steps
4. Calculation of the convergent flow solution, in accordance with all three equations, supersonic conditions
5. Set up the optimization problem with the initial values of constrains and the step size.

The main purpose is to obtain an optimum shape for airfoil for a maximum lift drag coefficient. The initial profile's thickness to chord ratio was selected to be small in order to compare the obtained results with those from the linear theory. The geometric constrains were imposed on the trailing edge, minimizing the thickness as to avoid the convergence to the trivial and non-practical shapes, as plate airfoil.

The domains were decomposed into 4 blocks as to reduce the required memory for the flow equations and sensitivity analysis. In order to locate the shocks and other flow characteristics a preliminary domain of  $165 \times 35$  grids was generated with a circular outer boundary surrounding the leading edge of the profile. Observing the computer flow field, a second grid was created with different dimensions of the cells, but with the outer boundary moved in to be just a few cells upstream of the bow shock. This grid was normally clustered to the airfoil surface, as to capture the boundary layer, and further clustered when the shock was expected.

All of the boundary conditions used have been applied explicitly. The boundary conditions are implemented using one layer of phantom points outside of the computational field, which results in a first order in space extrapolation at the boundaries and enhances the vector computer code. The phantom points at far fields are set to enforce a certain condition (supersonic or subsonic inflow or outflow) at the cell face, which is on the boundary, while at solid surfaces they are set to enforce the no-slip condition.

The changes in dependent variable are set equal to zero for all boundaries except for the block boundaries. The characteristics for the variable boundary conditions are designed to allow information concerning the flow into or out of the computational field as dictated by the signs of the Eigen values. The optimizer should automatic detect the adverse pressure gradient due to the extensive expansion around the leading edge, hence improving the profile efficiency. The positioning of the stagnation point on the lower surface, followed by an expansion of the flow around the leading edge was deemed sufficient to examine the problem for the argument set for the present study.

## VI. CONCLUSIONS

Comparing the subsonic and supersonic flow, at supersonic Ma numbers, the drag characteristics are generally higher than in subsonic.

The normal force and the pitching moment for the supersonic profiles have the maximum located at 0.7-chord length, by difference with the subsonic, where the maximum is located at 0.3-0.4 chord length.

At the leading edge for the supersonic profiles are different rolling vortices. By imposing an extended separated flow over that zone of the airfoil, appears an increase in the normal force. By supplementing the wing with flaps, the flow phenomenon has an appreciable effect on the maximum lift coefficient for the supersonic airfoils at high subsonic and supersonic Ma numbers.

It is not necessary to avoid the supersonic flow as to have high transonic drag coefficient. By keeping the maximum local Mach number smaller than 1.2 and if the maximum speeds is forward of the airfoil "crest", a low drag force with some supercritical flow can be used. For efficient functioning it is necessary to keep on the upper surface  $C_p$  highly enough, as to realize positive pressures on the lower surface. This can be done easily near the trailing edge. This technique of loading together with minor changes at the airfoil nose can lead to reasonable low drag force at high Mach numbers.

In the present paper, some corrections were made for the transonic speeds. The idea of carefully calculating the section where local supersonic flow is obtained without shockwaves (shock-free sections) has been a challenge. Too much loading can produce large negative pitching moments with trim drag and structural weight penalties. The adverse pressure gradient on the extrados can produce separation in extreme cases.

The thin trailing edge may be difficult to manufacture, but for supersonic flow, it represents a necessary condition. Appearance of a high force is quite common, a situation when the substantial drag section coefficient increases with the Mach number.

For all profiles the numerical simulations were accomplished for  $Ma = 0.8$  and  $Mach = 1.1$ , with an attack an-

gle of  $0^\circ$ ,  $2^\circ$ ,  $4^\circ$ . There where selected 36 points on profile, 18 on the extrados and 18 on the intrados. This type of set was critical in mitigating the negative volume problems in grid regeneration during the optimization process. The present study also demonstrates the possible difficulties in solving such optimization problems.

The convergence criteria was set at 50 iterations for the second condition, if three consecutive iterations have as results a difference smaller than 0.001 for objective function, which includes 6 gradient updates (for sensitivity analysis and flow analysis). All calculations were obtained using a numerical grid with  $221 \times 40$  points.

Large effort was expended to generate an orthogonal grid as possible at the airfoil surface, since the mentioned scheme is very sensitive at this aspect. The spacing set for the first point of the body was 0.000001 which gave approximately 15-20 grid cells inside the boundary layer and resulted in a minimum  $y$ , less than over the entire airfoil. The entire grid was oscillated as a rigid body. The idea of using sub-iterations for unsteady calculations was used as to improve the convergence of the solution at each time step and to allow larger sizes of time steps.

Near the leading edge, the large compression of the lower surface was largely reduced, and the expansion of the upper surface was slightly increased. The leading edge angle was reduced as to decrease the wave drag. The leading edge shock angle was also reduced, having as immediate effect an increasing of the optimized coefficient of pressure. For the first two profiles, the optimizer did not shift the  $t_{max}$  exactly to the mid-chord, but in the last two it achieved the objective by reducing  $t_{max}$  without shifting  $x_{tmax}$  from the mid-chore.

The predicted steady-state solution for the flow characteristics of the initial section was considered as initially desired: the stagnation point at the lower surface resulting in a very low pressure bubble near the leading- edge.

The optimizer evaluated the first search direction based on the objective function. The leading edge started to shift downward to align the upper surface with the oncoming flow, while the curvature of the lower surface near the trailing edge was changed to further compress the flow. The compression on the lower surface near the trailing edge was also increased.

## ACKNOWLEDGMENT

**Source of research funding in this article:** Research program of the Hydraulic machinery and Environmental Engineering Department financed by the University Politehnica of Bucharest.

*Received on September 18, 2017*

*Editorial Approval on November 6, 2017*

## REFERENCES

- [1] G. Drouge, Two-dimensional wings of minimum pressure drag, Theory of Optimum Aerodynamic Shapes, Chapter 5, *Academic Press, New York/London*, 1995.
- [2] A. Miele, A. Lusty, Second Order Theory for Optimum Two-Dimensional Wings, Theory of Optimum Aerodynamics Shapes, Chapter 9, *Academic Press, New York/London*, 1999.
- [3] L. G. Pitman, Supersonic Airfoil Optimization, *Journal of Aircraft*, Vol. 24, No.12 pp. 873-879, 1997.
- [4] M. J. Mann, H. W. Carlson, Aerodynamic design of Supersonic Cruise Wings with a Calibrated Linearized Theory, *Journal of Aircraft*, Vol. 31, No.1 pp. 35-41, 2004.
- [5] R. M. Kulfan, A. Sigalla, Real Flow Limitation in Supersonic Air-

- planes Design, *AIAA Paper* 78-147, 1989[6] V. Radulescu, Hydrodynamic theory for isolated and into cascade hydrodynamic profiles, *Publisher Bren, Series Hydraulics*, Bucharest, 2004, ISBN 973-648-279-0.
- [7] Victorița RAdulescu, I. Seteanu, A. Radulescu, Steady Flow Over a Finite Hydrofoil, *Conf. CEEX, Brasov, Romania*, iulie 2008
- [8] O. Baysal, M.E. Eleshaaky, Aerodynamic Design Optimization using Sensitivity Analysis and Computational Fluid Dynamics, *AIAA Journal*, Vol. 30, No. 3, pp 718-725, 1992
- [9] C. C. Item, Wing Section Optimisation for Supersonic Viscous flow, M.S. thesis, Aerospace Engineering Department, *Old Dominion University, Norfolk*, 1999
- [10] V. Radulescu, Rotational and potential flows, 250 pgs., *Publisher Bren, Series Hydraulics, Bucharest*, 2004, ISBN 973-648-280-2
- [11] S. M., Rufen, A. Gupta, and D. Marshall, Supersonic channel airfoils for reduced drag, *American Institute, Aeronautics & Astronautic*, 2000, 38(3), pgs. 480- 486.